SOL-GEL TEMPLATE ASSISTED SYNTHESIS AND UP-CONVERSION PROPERTIES OF (Yb-Er) DOPED SiO$_2$-LiYF$_4$ GLASS CERAMIC RODS

C.E. SECU[*], E.MATEI

National Institute of Materials Physics, P.O. box MG-7, Bucharest-Magurele, 077125, Romania

Up-conversion properties of the glass-ceramics microrods containing (Er^{3+},Yb^{3+})-doped LiYF$_4$ nanocrystals have been studied. Under 980 nm laser light pumping, both Yb^{3+}/Er^{3+} co-doped LiYF$_4$samplesshow green (($^2H_{11/2}$, $^4S_{3/2}$) → $^4I_{15/2}$) and red ($^4F_{9/2}$ → $^4I_{15/2}$) up-conversion luminescences explained by a two-photon processes. The luminescence decay time of the green luminescence is much shorter in the glass-ceramics microrods (0.9μs) compared to the bulk powder (15μs) indicating the enhancement of the non-radiative relaxation rate due to the cross-relaxation effects between Er^{3+}-ions. The quantum efficiencies were estimated for the green luminescence being much smaller in the glass-ceramic rods ($\eta = 0.15\%$) compared the bulk powder ($\eta = 2\%$) or pellet ($\eta = 46\%$).

1. Introduction

One-dimensional nanostructures such as nanorods, nanowires, and nanotubes can be used for the efficient transport of electrons and optical excitations and sustain the next generation of optoelectronic nanodevices [1]. Due to their diameters below the wavelength of light and the high aspect ratio, nanowires can act as efficient light waveguides linking individual components to form complex networks [2,3], optoelectronic nanodevices [4] and nanowire lasers [5].

Sol-gel template assisted technique has been provided a new general route for preparing one-dimensional nanostructures (nanowires) [6] by conducting sol-gel synthesis within the pores of various micro- and nanoporous template membrane ([7] and references therein). The method is based on the filling the nanopores of a membrane (anodic alumina or etched ion track membranes) with a certain material, which adopts the exact shape of the hosting pore followed by the membrane removal and material densification by calcination at elevated temperatures. The method has been used to prepare luminescent nanostructures like Eu^{3+}-doped LaPO$_4$ [8], Eosin doped silica rods [9], dye-doped KAP and KDP nanorods [10] or glass ceramic silica rods containing Eu^{3+}-doped LiYF$_4$ nanocrystals [11].

The aim of the paper is to study and to characterize the up-luminescence properties (i.e. near-infrared (NIR) conversion into the visible spectral range) of the glass-ceramics microrods containing (Er^{3+},Yb^{3+})-doped LiYF$_4$ nanocrystals by comparison to the corresponding bulk powder.

2. Experimental

For the preparation of the Yb^{3+}(4%)doped (1%) (95SiO$_2$–5LiYF$_4$) (mol%) xerogels and glass-ceramic rods we used synthesis from liquid solution of organometallic tetraethylorthosilicate (TEOS) precursor corresponding to a chemical reaction implying metal alkoxides and water in an

---

[*] Corresponding author: cesecu@infim.ro

alcoholic solvent [12]. In the first step tetraethoxysilane (TEOS) was hydrolyzed under constant stirring with a mixed solution of ethanol and water and using glacial acetic acid as catalyst; molar ratio was 1:4:10:0.5. Then another solution of $Er(CH_3COO)_3$, $Yb(CH_3COO)_3$, $Y(CH_3COO)_3$, $Li(CH_3COO)$ and CF_3COOH with the molar ratio for Er:Yb:Y:Li:F of 1:4:5:20:179was prepared by and added to the first solution was prepared by and added to the first solution, followed by stirring for 1 h at room temperature. The liquid sol was allowed to fill the pores of a track etched polycarbonate membrane (30μm thickness, 1μm pore diameter and 10^8 cm^{-2} pore density) [11] used as template and then kept at room temperature for aging and strengthening. Then the membrane was dissolved in dichloromethane and the solution deposited on quartz slides. In order the obtain glass ceramic microrods we annealed the slides at 530 ^{o}C in air as resulted from thermal analysis measurements [12].

The morphology of the samples was studied by using a Carl Zeiss EVO 50 scanning electron microscope (SEM) equipped with energy dispersive X-ray analysis (EDX) for the elements distribution characterization; the samples were placed on stabs using adhesive carbon discs.

Photoluminescence (PL) and lifetimes measurements have been performed at room temperature by using a commercial Jobin Yvon spectrophotometer Fluoromax 4-P; the spectra were corrected with the spectral sensitivity. For the power dependence of the up-conversion (UC) luminescence intensity we used a laser diode module centered at 980nm with a maximum power of 2.3W.

3. Results and discussion

3.1. Scanning electron microscopy (SEM)

In the Figure 1 are depicted the SEM images of the glass ceramic microrods recorded at two different magnifications. We have observed an uniform distribution of microrods of about 0.8μm diameter and 10 μm length showing nanostructures of about 60-70nm inside them.
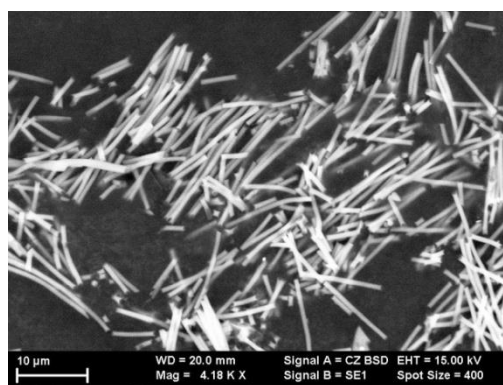
Fig. 1. SEM image of the glass-ceramic microrods.

Supposing a similar fluoride nanophase precipitation mechanism in both glass ceramic bulk powder and microrods (based on of Li and Y-trifluoacetates thermal decomposition [12]) we assign the nanostructures to the presence of the $LiYF_4$ nanocrystals (Figure 1).
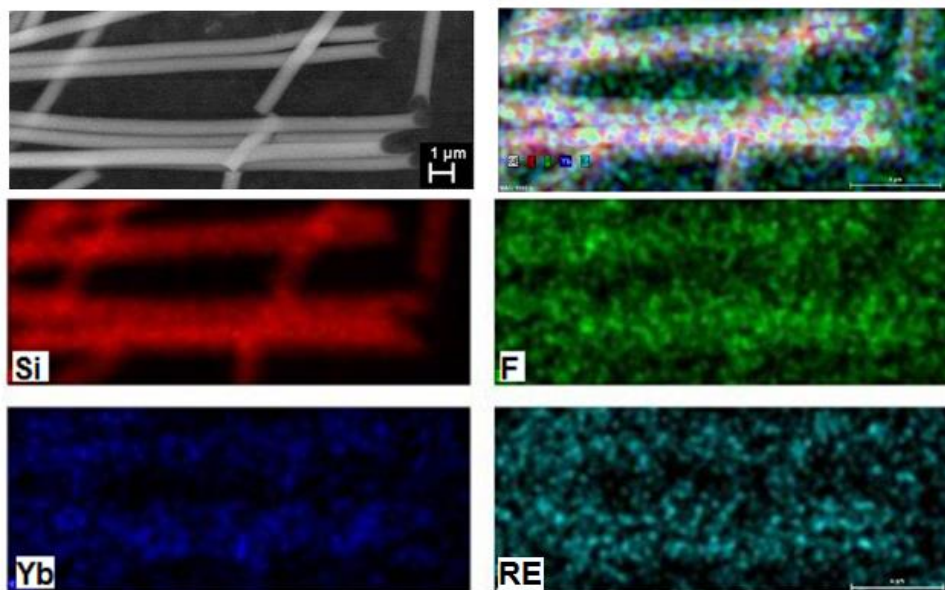
Fig. 2. SEM image of the glass-ceramic microrods by comparison to the elements distribution obtained by the EDX measurements (RE=Er^{3+}).

As can be observed in the Figure 2 elements distribution characterization has shown a uniform distribution of the elements within the microrods.

3.2. Photoluminescence decay

Time decay profile of the 550nm luminescence band (($^2H_{11/2}$, $^4S_{3/2}$) $\rightarrow$ $^4I_{15/2}$) were recorded under 378nm excitation for both Yb^{3+}/Er^{3+} co-doped glass-ceramics bulk powder and microrods(Figure 3). For the bulk powder the curve has been relatively well fitted with single exponential decay of about 15±0.05μs. For the rods the curve is not exponential and we have computed an effective decay time of about 0.9±0.05μs; both lifetimes values are dramatically shortened compared to the polycrystal (340μs) [13].
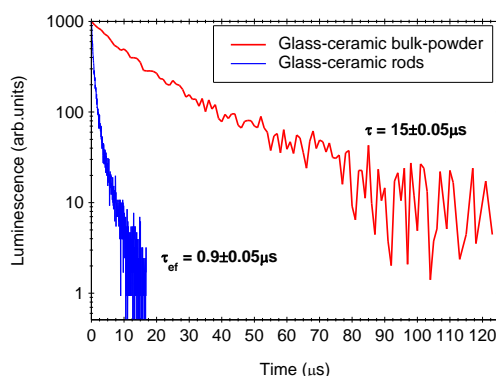
Fig. 3. Photoluminescence decay curves of the 550nm luminescence under 378nm excitation for Yb^{3+}/Er^{3+} co-doped glass-ceramics bulk powder and microrods represented in logarithmic scale

3.3. UP-conversion luminescence

Under 980nm laser light pumping both Yb^{3+}/Er^{3+} co-doped LiYF$_4$glass-ceramic rods and bulk powder show green and red luminescences (Figure 4), assigned to the ($^2H_{11/2}$, $^4S_{3/2}$) $\rightarrow$ $^4I_{15/2}$and ($^4F_{9/2} \rightarrow {}^4I_{15/2}$) transitions of the Er^{3+} ions [14].
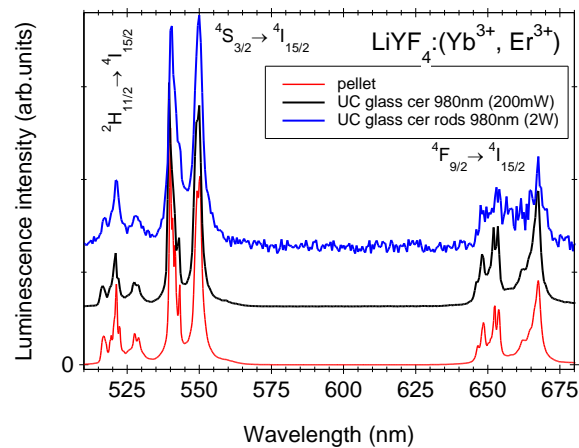
Figure 3. Green ($^2H_{11/2}$, $^4S_{3/2}$ → $^4I_{15/2}$) and red ($^4F_{9/2}$ → $^4I_{15/2}$) Er^{3+} up-conversion luminescences excited at 980 nm in Yb^{3+}-Er^{3+}-doped oxyfluoride glass-ceramic rods and bulk powder samples by comparison to the (Yb,Er)-doped LiYF$_4$polycrystal sample.

The luminescence bands and their splitting in the glass-ceramic bulk powder and microrods are almost identical indicating that Er^{3+} ions are embedded dominantly inside the LiYF$_4$ nanocrystals [12].

In order to investigate the UC mechanisms, the pump power dependencies of the green ($^2H_{11/2}$, $^4S_{3/2}$) → $^4I_{15/2}$and red ($^4F_{9/2}$ → $^4I_{15/2}$) emissions for the glass ceramic rods were measured. It is known that at the unsaturated condition, the UC luminescence intensity is proportional with the nth power of the incident pump power, where n is the number of the pumping photons required to excite RE ions from the ground state to the emitting excited state [19]. The power dependence for the UC emissions in a double logarithmic plot is shown in Fig. 4 where n is the slope of this dependence. In the present case, the slopes for both green and red emissions indicate that two photons are involved in the UC mechanism (Figure 5).
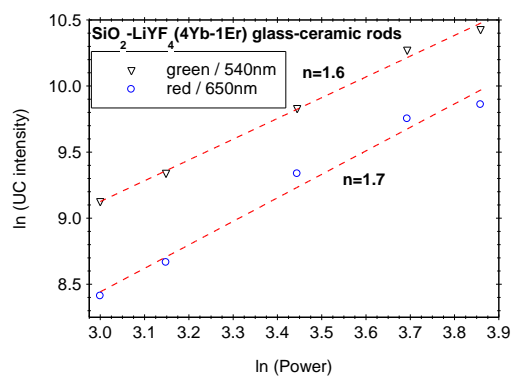
Fig. 4. Double logarithmic plot of luminescence intensity vs. incident laser power for green (($^2H_{11/2}$, $^4S_{3/2}$) → $^4I_{15/2}$) and red ($^4F_{9/2}$ → $^4I_{15/2}$) up-conversion luminescence recorded on Yb^{3+}/Er^{3+} co-doped oxyfluoride glass-ceramic rods.

The UC luminescence mechanism for Yb^{3+}/Er^{3+}doped LiYF$_4$ nanoparticles has been extensively investigated [12,15-17] and therefore we do not address it in detail here.
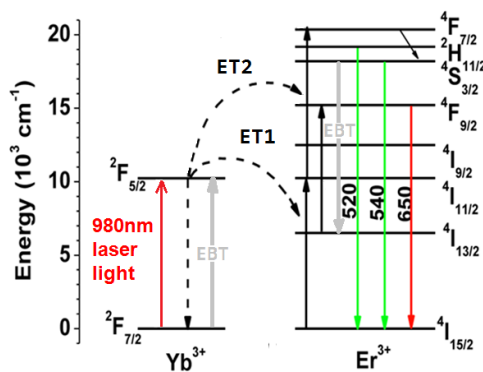
Fig. 5. Energy level schemes of Yb^{3+} and Er^{3+} and the main energy transfer processes from Yb^{3+} to Er^{3+} represented by curved dashed arrows.

Under 980 nm laser light pumping the green emitting levels ($^2H_{11/2}$, $^4S_{3/2}$) are populated by the Yb^{3+} - Er^{3+}ET1 [$^2F_{5/2}$ (Yb^{3+}) + $^4I_{15/2}$ (Er^{3+}) $\rightarrow$ $^2F_{7/2}$ (Yb^{3+}) + $^4I_{11/2}$ (Er^{3+})] and ET2 [$^2F_{5/2}$ (Yb^{3+}) + $^4I_{11/2}$ (Er^{3+}) $\rightarrow$ $^2F_{7/2}$ (Yb^{3+}) + $^4F_{7/2}$ (Er^{3+})] processes (Figure.8), followed by the rapid multiphonon (MP) transition $^4F_{7/2} \rightarrow {}^2H_{11/2}$. The lower emitting levels are then populated via multiphonon and cross-relaxation (Yb^{3+}-Er^{3+}) processes followed by the green (($^2H_{11/2}$, $^4S_{3/2}$) $\rightarrow {}^4I_{15/2}$) and red ($^4F_{9/2} \rightarrow {}^4I_{15/2}$) emissions (Figure 5) [18].

The substantial role played by the non-radiative relaxation processes in glass ceramic rods and bulk powder can be clearly observed from the PL decay measurements. The emission quantum efficiency of the emitting level is given by: $\eta = A_{rad} / A_{tot}$ where $A_{tot} = 1/\tau = A_{rad} + A_{nrad}$ (and τ is the observed lifetime).By using the calculated probability (A_{rad}) of the 540nm radiative transition of 1375 s^{-1} [20], we computed the quantum efficiency of the transition which is much smaller in the glass-ceramic rods ($\eta = 0.15\%$) compared the bulk powder ($\eta = 2\%$) or polycrystal ($\eta = 46\%$).

The radiative decay rate of the transition is the same in the Yb^{3+}/Er^{3+} co-doped glass-ceramic bulk powder or rods. Therefore it was supposed that in the bulk powder the non-radiative decay rate enhanced through energy back-transfer (EBT) from Yb^{3+} to Er^{3+} [12] (Figure 5) and the cross-relaxation processes caused by Er^{3+}-ions pairing [18,21]. As the cross-relaxation processes between interacting RE^{3+}-ions manifest through a non exponential shape of the luminescence decay curve(which is almost exponential – Figure 3) it is reasonable to suppose that Yb^{3+}-Er^{3+} back-transfer is the dominant effect responsible for the luminescence quenching. In addition, a high concentration of surface atoms and defects [17,22] on the LiYF$_4$ nanocrystals surface and hydroxyl ions (OH^{-1}) [23] may act as effective non-radiatively decay chanels. In the glass-ceramic rods there are additional non-radiative relaxation mechanisms competing with the radiative decay rate that cause further reduction of the luminescence decay time and of the luminescence efficiency. As the luminescence decay curve has an obvious non exponential shape (Figure 3) it indicates enhancement of the cross-relaxation processes caused by Er^{3+}-ions pairing due to the high local concentration of these ions [11]. This effect might be related to the influence of the dimensional constraints imposed by the membrane pores during xerogel formation and subsequent glass ceramization.

4. Conclusions

Up-conversion properties of Yb^{3+}/Er^{3+} co-doped LiYF$_4$ nanocrystals in glass-ceramics have been studied by comparison to the corresponding bulk powder. Under 980 nm laser light pumping we have observed up-conversion luminescence green (($^2H_{11/2}$, $^4S_{3/2}$) $\rightarrow {}^4I_{15/2}$) and red ($^4F_{9/2} \rightarrow {}^4I_{15/2}$) bands due to the Er^{3+} ions. Laser pump power dependencies of UC luminescence intensities show a quadratic laser power dependence indicating a two-photon process. In the glass-

ceramic rods green luminescence decay time(0.9μs) is much shorter compared to the bulk powder (15μs) due to the enhancement of the cross-relaxation between Er^{3+}-ions; the quantum efficiencies were estimated for the green luminescence being much smaller in the glass-ceramic rods ($\eta = 0.15\%$) compared the bulk powder ($\eta = 2\%$).

Acknowledgements

References

[1] Y. Xia, P. Yang, Y. Sun, Y. Wu, B. Mayers, B. Gates, Y. Yin, F. Kim, H. Yan, Adv. Mater. **15**, 353 (2003).

[2] C. Barrelet, A. Greytak, C. Lieber, Nanowire Photonic Circuit Elements, Nano. Lett. **4**,1981 (2004)

[3] D. J. Sirbuly, M. Law, J. C. Johnson, J. Goldberger, R. J. Saykally, P. Yang,Science **305**, 1269 (2004).

[4] X. Duan, Y. Yang, Y. Cui, J. Wang, and C. Lieber, Nature**409,** 66 (2001)

[5] M.A. Zimmler, F. Capasso, S. Müller and C. Ronning, Semicond. Sci. Technol. **25,** 024001(2010)

[6] Brinda B. Lakshmi, Peter K. Dorhout, Charles R. Martin, Chem. Mater. **9**,857 (1997)

[7] Guozhong Cao, Dawei Liu, Adv. Colloid Interface Sci. **136**,45 (2008)

[8] Mary J. Fisher , Wehzhong Wang , Peter K. Dorhout, Ellen R. Fisher, J. Phys. Chem. C **112,** 1901(2008)

[9] M. Secu, C.E. Secu, M.Sima, R.F. Negrea, C. Bartha, M. Dinescu, V. Damian, J. Lumin. **143**, 89 (2013).

[10] M.Enculescu and C.Trautman Radiat.Meas. **45**, 602 (2010).

[11] C.E. Secu, M. Secu Opt Mater, **47**, 95 (2015)

[12] C.E. Secu, R.F. Negrea, M. Secu, Opt. Mater. **35**, 2456 (2013).

[13] M. Secu, C.E. Secu Journal of Non-Crystalline Solids**426**, 78 (2015)

[14] J. P. Wittke, I. Ladany and P. N. Yocom J Appl Phys**43**(2), 595 (1972).

[15] Xiangyu Zhang, Minqiang Wang, Jijun Ding,Xiaohui Song,Jing Liu, Jinyou ShaoYajing Li,RSC Adv.**4**40223 (2014).

[16] Liming Zhang, Zhixin Wang, Zhuoxuan Lu, Kai Xia, Yan Deng, Song Li, Chuanxiang Zhang, Yuanfu Huang, and Nongyue He, J. Nanosci. Nanotechnol.**14**, 4710 (2014).

[17] XiaojieXue, Shinya Uechi, Rajanish N. Tiwari, ZhongchaoDuan, Meisong Liao, Masamichi Yoshimura, Takenobu Suzuki, and YasutakeOhishi, ,Opt. Mater. Express **3**(7), 989 (2013).

[18] S. Georgescu, A.M. Voiculescu, C. Matei, C.E. Secu, R.F. Negrea, M. Secu, J. Lumin. **143**,150 (2013).

[19] M. Pollnau, D. R. Gamelin, S. R. Lüthi, H. U. Güdel, Phys. Rev. B **61**,3337 (2000).

[20] A. M. Tkachuk, I. K. Razumova, A. A. Mirzaeva, A. V. Malyshev and V. P. Gapontsev, Optics and Spectroscopy **92**(1),67 (2002).

[21] FiorenzoVetrone, J. Christopher Boyer, John A. Capobianco, Adolfo Speghini, Marco Bettinelli, J. Phys. Chem. B, **107**(5), 1107 (2003).

[22] M. Secu, J Nanopart. Res. **13,** 2727 (2011).

[23] C.E. Secu, C. Bartha, S. Polosan, M. Secu, J. Lumin**146**, 539 (2014).